Simulation and Testing of Transducers for Lamb Wave Generation

J.H. Nieuwenhuis[1,2], J. J. Neumann,[3] D.W. Greve,[3] and I.J. Oppenheim[4]
[1] Institute of Sensor and Actuator Systems, Vienna University of Technology, Austria
[2] Bosch Research and Technology Center North America, Pittsburgh, PA, USA
[3] Department of Electrical and Computer Engineering, Carnegie Mellon University, Pittsburgh, PA, USA
[4] Department of Civil and Environmental Engineering, Carnegie Mellon University, Pittsburgh, PA, USA

ABSTRACT

Ultrasonic Lamb waves are used to detect flaws in plates, and in our work PZT wafers are used both to transmit and receive the waves. Multiple wave modes can exist, which in combination with pulse dispersion can make it difficult to interpret pulse-echo response. Using an appropriate pulse train, we seek to achieve selective generation of the S0 wave in order to distinguish it from the A0 wave and to avoid the generation of waves in higher modes. We present two-dimensional FEM transient simulations of the source region, we compare those observations to available analytical results, and we show how those results can guide a designer in choosing transducer dimensions for mode selectivity. We then show parallel experimental results and compare the measured and predicted response. In our simulations and experiments the dimensions of the PZT wafer transducer are 0.64 x 6.4 x 19.2 mm, and the thickness of the aluminum plate is 1.59 mm; excitation frequencies used in our simulations and experiments are typically in the range of 33 to 800 kHz.

I. Introduction

Lamb waves can be used for non-destructive testing of aluminum aircraft panels, composite panels, and other plate-shaped objects. Complications that are encountered in applying Lamb waves include the existence of multiple modes and the dispersive character of the modes. A partial solution to this complexity is the use of transducers that excite only a single mode. Approaches for selective excitation include angled prisms [1], comb-type transducers [1,2,3] or linear arrays with time-delayed excitation [4,5]. There has been recent interest in the use of single PZT wafers as transducers, in part because of the simplicity and potentially low cost of these transducers. Single PZT wafers have been explored with continuous sinusoidal excitation [6,7] or pulsed excitation [8,9] for defect detection in composite panels, and the influence of flaws on the Lamb waves has been modeled. Some authors [6,8] have recommended use of the A0 mode because of lower attenuation. Alternately, selective excitation of the S0 mode has also been proposed and demonstrated [9]. A theoretical explanation for the mode selectivity of the PZT wafer transducer has been reported [9], although that analysis is strictly applicable only to the sinusoidal steady state and makes numerous simplifying assumptions.

In this paper, we combine finite element simulation and experimental studies to explore further the operation of the wafer transducer. We separately model the emission and detection processes. In particular, we have calculated the wave velocities and the received voltage signals due to A0 and S0 modes at an output transducer as a function of pulse center frequency. These calculations include the effects of finite pulse width, pulse dispersion, and the detailed interaction between the piezoelectric element and the transmitting medium. The results obtained provide more accurate predictions of the mode selectivity than have been previously reported using the simplified point-force model [9].

II. Observations of mode selectivity

Figure 1 shows the plane strain geometry considered in this work. Two wafer-type transducers 0.064 cm $\times$ 0.64 cm $\times$ 1.92 cm in size ($t \times 2a \times$ depth into page) were bonded to a 1.59 mm thick aluminum plate using Epotek E4110-LV silver epoxy. The transducers were made from Motorola 3203HD PZT, with the poling direction normal to the plate surface. The emitting transducer was driven by a windowed sinusoid of the form

$$V(t) = \begin{cases} V_0 \sin(wt) \cdot \left(\sin(\frac{wt}{10}) \right)^2 & t < \frac{10p}{w} \\ 0 & otherwise \end{cases}$$

where V_0 was 5 volts and the center frequency was varied from ($w/2p$ =) 33 kHz to 800 kHz. The exciting waveform was generated by a National Instruments PCI-5411 and the received pulse was recorded using a National Instruments PCI-5112 100 MHz A/D board. Typically 5000-10000 samples were acquired under computer control using Labview.

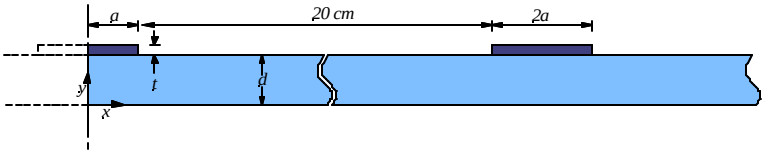

Fig. 1. Geometry, plane strain, for PZT wafer experiments and simulations; symmetrical about y-axis.

Pulse transients received in experimental studies are shown in Fig. 2, for t < 150 μsec, for several selected frequencies. Two distinct pulses are visible. The first pulse is due to the S0 emitted mode and is received at a time which is almost independent of frequency. The second pulse is from the A0 mode, shows significantly more dispersion, and exhibits a frequency-dependent group velocity. This pulse behavior is consistent with the calculated dispersion curves for aluminum.

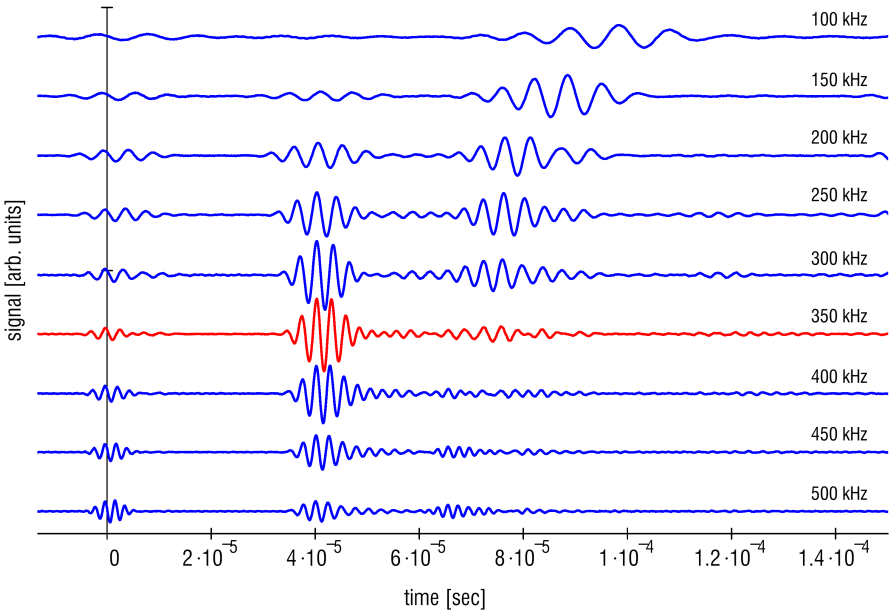

Fig. 2. Received signals (experimental, 20 cm separation) as a function of frequency.

Also apparent in this data is a strong dependence of pulse amplitude on frequency. In particular, the S0 mode has a maximum near 350 kHz and at this frequency the A0 mode has low, though nonzero, amplitude. This selectivity of wafer-type transducers was previously reported by Giurgiutiu [9]. His mathematical model used a steady state sinusoidal point force excitation, acting in the x-direction and applied to the plate at $x = a$, to replace the transducer. It was shown [9] that the peak and minimum frequencies were given by

$$f_{\min}^{i,n} = \frac{v_{phase} \cdot n}{2a} \quad \text{and} \quad f_{\max}^{i,n} = \frac{v_{phase} \cdot (n + \tfrac{1}{2})}{2a}. \qquad (1)$$

The point-force model with steady state sinusoidal excitation is a considerable simplification of the interaction between the PZT transducer and the plate. We present the results of finite element simulations which (1) account accurately for all the forces exerted on the plate by the PZT transducer, (2) model separately the emission and detection of ultrasonic waves by PZT transducers, and (3) calculate the response under realistic, transient pulses.

Simulation of Lamb wave excitation

Emission simulations were performed using the time-stepping mode of the two-dimensional plane strain mode of FEMLAB 2.3 (ode23s solver). In all simulations reported below, the plate was aluminum (Young's modulus E = 70 GPa, r = 2.7 gm/cm^3, Poisson's ratio $?$ = 0.33, mass damping coefficient 0, stiffness damping coefficient = 0). These dimensions were chosen to match the configuration used in experiments described above.

A simplified model of the PZT wafer transducer was developed for emission simulation in order to avoid the need for a full multiphysics model. (In subsequent simulations the results are compared to those obtained from a full "end-to-end" multiphysics simulation.) Consider a free PZT wafer, unbonded but under conditions of plane strain, subjected to a voltage $V(t)$ at its electrodes producing an electric field E_y; in this configuration, y is both the through-thickness direction and the poling direction. Strains S are calculated from plane strain condition as

$$0 = c_{11}S_x + c_{13}S_y - e_{31}E_y$$
$$0 = c_{13}S_x + c_{33}S_y - e_{33}E_y$$

where quantities c_{11}, c_{13}, c_{33}, e_{31} and e_{33} are material constants for the PZT material; throughout this paper the tensor notation and convention for piezoelectric modeling is employed. The resulting strains are equal to the strains that would be caused by forces $e_{31}E_y$ per unit area applied to the right and left faces, and forces $e_{33}E_y$ applied to top and bottom surfaces of the PZT wafer. In our simulation, a PZT wafer with its appropriate elastic and inertial properties was bonded to the aluminum plate, and forces as discussed above were applied to the coupled system at the boundaries of the PZT wafer. In this manner, the effect of the applied voltage and the coupled behavior of the transducer and plate (the PZT and the aluminum) were incorporated [10].

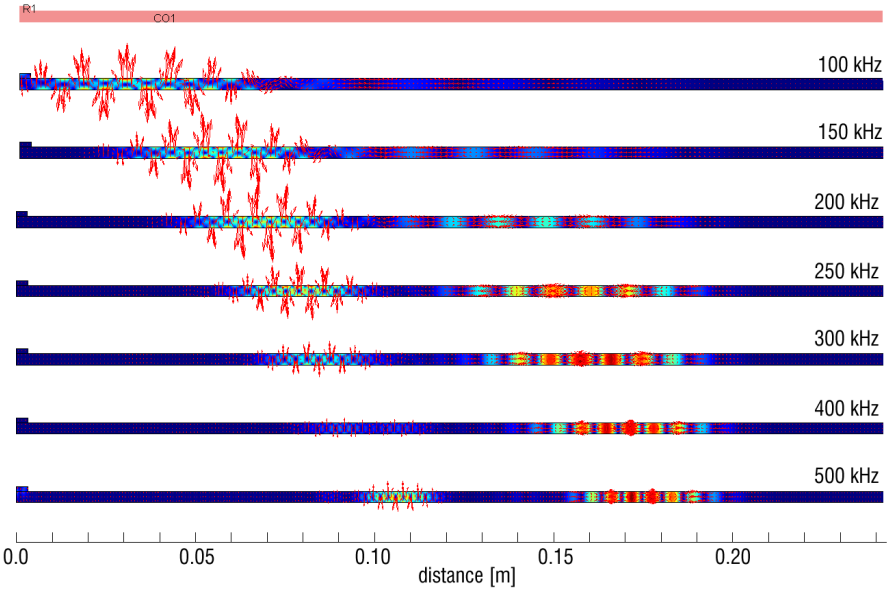

Fig. 3. Emission of A0 and S0 waves, at t = 40 μs. The propagation velocity of the A0 mode increases with frequency, and the emitted intensity reaches a minimum near 400 kHz. (Plate thickness exaggerated 2X.)

Figure 3 shows results, at time $t = 4 \times 10^{-5}$ sec, from simulations at a range of frequencies between 100 KHz and 500 kHz. The wave is generated at the left edge and propagates to the right. The colors in this figure indicate the von Mises stress. The arrows indicate the vector particle displacements from the equilibrium position.

We see the two propagating modes to display clearly different characteristics. The S0 mode has the highest group velocity and shows particle displacements mostly in the x direction, along the direction of propagation. There is a small dilation and expansion in the y direction, which is symmetric about the center of the plate; this arises due to the Poisson effect. The slower wave is the A0 mode, which shows particle displacements that are mostly in the y direction and are asymmetric about the center of the plate. The propagation velocity of the A0 mode is less than that of the S0 mode and depends significantly on frequency. Qualitatively, it appears that the relative magnitudes of the A0 and S0 modes vary, with a minimum in the A0 mode amplitude near 400 kHz.

To quantify the variation in the wave magnitudes with frequency, we have determined the maximum value of the x component of velocity v_x for the S0 mode and the maximum value of v_y for the A0 mode. These are plotted in Fig. 4 as a function of frequency. We see a minimum in the amplitude of the A0 mode, near 400 kHz, two peaks in the A0 mode, near 180 and 600 kHz, and a peak in the S0 mode, near 400 kHz. These results are qualitatively similar, but not identical to, the earlier predictions [9] of the point force model. The important differences are (1) a shift of the peaks and minima to somewhat higher frequencies and (2) relatively stronger emission of waves at high frequencies than observed with point-force excitation. We continue to observe an optimum frequency at which the S0 mode is predominantly emitted.

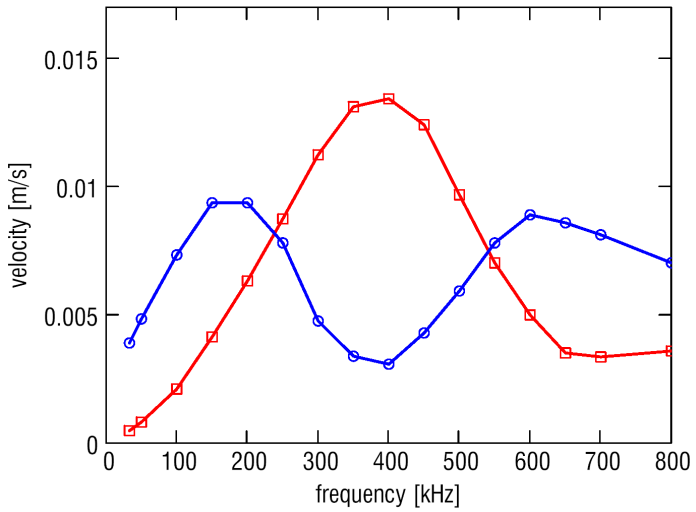

Fig. 4. Maximum particle velocity of generated waves as a function of frequency for the A0 mode (circles) and the S0 mode (squares), simulated using the PZT model with a driving voltage of 10 volts peak-to-peak.

III. Detection of Lamb waves

We now consider the detection of Lamb waves. Because this is the inverse process of wave generation, it may appear at first thought that the wave generation and wave detection curves should be the same. However, this is not the case. In contrast to wave generation, for detection a decrease in signal is not expected at frequencies where the size of the element is shorter than a half wavelength. At these frequencies the detection is expected to show constant sensitivity, since there is no partial cancellation as is the case in the wave generation. This difference necessitates a separate analysis of wave detection.

In order to analyze the detection of Lamb waves we used a full electro-mechanical (multiphysics) simulation. These simulations were performed using the multiphysics (electrostatics plus plane-strain structural mechanics) time-dependent mode of FEMLAB 3.0, using the Direct (UMFPACK) linear solver in the weak mode. The response of a receiving PZT was calculated separately for S0 and A0 modes. Each mode was selectively generated by two point forces acting at on the top and bottom of the aluminum plate. When these two sources are

driven in phase the S0 mode is launched, and when driven out of phase the A0 mode is launched. The bottom surface of the receiving PZT was electrically grounded ($V = 0$) and an equipotential boundary condition was imposed on the top surface. The simulation yields the time-dependent mechanical displacements and also the time-dependent potential of the PZT top surface. The sensitivity for each mode was calculated by dividing the maximum top surface potential by the particle velocity for each wave.

Figure 5 shows the calculated receiver sensitivities as a function of frequency. At low frequencies the sensitivity of the PZT to the S0 mode is practically constant. In this frequency range the half-wavelength of the acoustic wave is longer than the PZT, and therefore the PZT functions as an ideal strain sensor. At higher frequencies the PZT is more than a wavelength long and the strain reverses sign along the transducer, therefore leading to a decrease in sensitivity.

The sensitivity of the PZT receiver to the A0 mode is very different, because strain is related to particle velocity by

$$S = \frac{du}{dt} = \frac{du}{dx}\frac{dx}{dt} = \frac{du}{dx}\frac{1}{c_p}$$

where S is strain, u is the particle displacement, and c_p is the phase velocity. The phase velocity of the A0 mode is strongly frequency-dependent, and decreases toward zero at low frequencies. Consequently, the A0 sensitivity increases strongly with decreasing frequency. We also see subtle evidence for the expected minimum in A0 sensitivity near 400 kHz where the transducer is exactly one wavelength long, and for the expected maximum near 600 kHz where the transducer is exactly 1.5 wavelengths long.

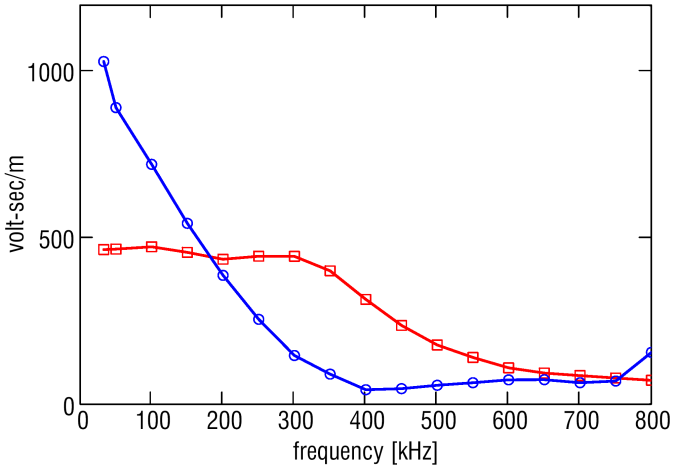

Figure 5. Simulated receiver sensitivity as a function of frequency: (circles) A0 mode and (squares) S0 mode.

In order to simulate the received signal amplitude for a given input pulse we multiply the particle velocity per volt (from Fig. 4) with the receive sensitivity in volts per unit particle velocity (Fig. 5). This yields the overall system transfer function v_{out}/v_{in} [volts/volt] which is shown in Fig. 6 as a function of the pulse center frequency. The S0 and A0 peak locations are near to the predictions of eqs. (1), with the S0 peak slightly lower in frequency and the A0 peak somewhat higher. For this geometry, generation of S0 is predicted to be strongly dominant near 325 kHz.

Also shown in Fig. 6 are individual data points comprising the predicted transfer function value, v_{out}/v_{in}, when both transmitter and receiver are simulated using a full multiphysics calculation. These “end-to-end” calculations are substantially more time-consuming, particularly at the extremes of high and low frequencies, and consequently we have performed these simulations only at a few selected frequencies. The results are in very good agreement with those obtained by simulating the receiver and transmitter separately. This further supports the accuracy of our PZT-equivalent force model for efficient simulation of wave emission.

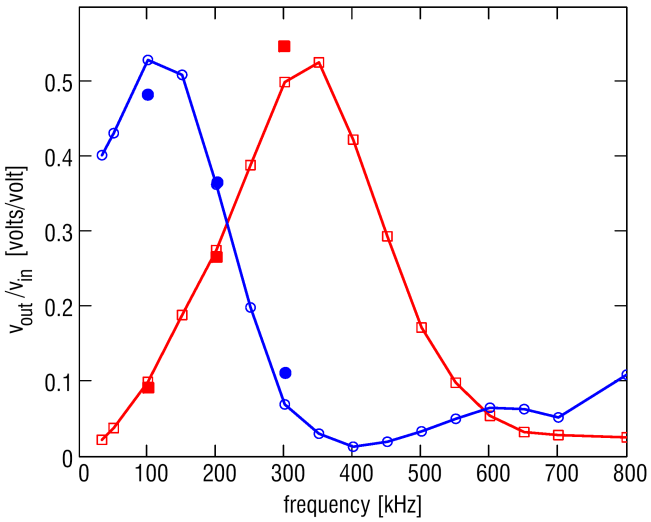

Fig. 6. Overall system transfer function v_{out}/v_{in} as a function of pulse center frequency: (■,□) S0 mode and (○,●) A0 mode. The solid points are the results from the full "end-to-end" multiphysics simulation.

IV. Comparison of simulations with experiment

Figure 7 shows the measured transfer function v_{out}/v_{in}, as a function of frequency, for three different tranducer pairs. For the S0 mode, we observe good agreement between experiment and simulation with respect to the position of the peak and the frequency dependence. Experimentally the peak S0 response is at 300-325 kHz, compared to the simulated peak, in Figure 6, near 350 kHz; the simple prediction from eq. (1) is 419 kHz.

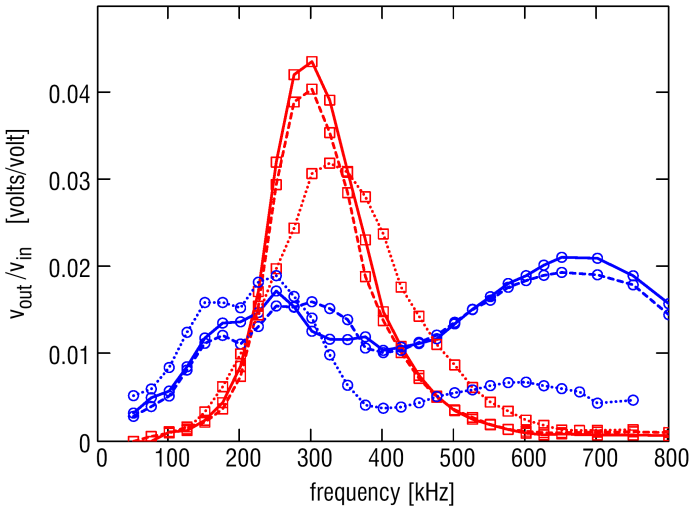

Figure 7. Measurements of the ratio of the peak output signal to the peak of the exciting pulse for three transducer pairs: (□) S0 mode and (●) A0 mode.

The agreement between experiment and simulation for the A0 mode is poor. The simulations predict a peak amplitude comparable to that of the S0 mode, whereas the observed peak of the A0 mode is much lower than that of the S0 mode. Moreover, the simulations predict a peak at a frequency near 100 kHz, whereas no peak is observed near that frequency in our experiments. Note, however, that the predicted peak frequency of approximately 100 kHz is in good agreement with eq. (1). Also, the predicted peak frequency near 100 kHz is in good agreement with measurements reported by Giurgiutiu [9], who employed a transducer close in length (0.7 cm compared to 0.64 cm) to the ones used in our experiments.

We have ruled out instrumental artifacts as an explanation for the discrepancy between simulations and experiment. Measurements with several different transducer pairs consistently show the same S0 peak position and also approximately the same S0 amplitude, whereas the A0 data shows significant variability.

We attribute the poor agreement of the A0 results to non-ideal bonding between the PZT wafer and the aluminum plate. This is supported by our observation of differences in the measured impedance spectrum (not shown) for different transducers, which is consistent with imperfect bonding. Seemingly the A0 mode is more sensitive to the bonding conditions than the S0 mode. We note that the published measurements by Giurgiutiu [9] show that results in better agreement with simulations can be obtained. In our opinion, the S0 mode may be preferable because it can be generated selectively and because it exhibits little dispersion over a wide frequency range.

V. Summary

In this paper, the operation of a PZT wafer transducer was analyzed for the generation and detection of guided acoustic waves using a combination of finite element simulation and experimental studies. The simulations account for the detailed mechanical interactions between the transducer and the transmitting medium, and in addition include a full multiphysics representation of the pulse reception.

The simulations and the experimental results demonstrate that a piezoelectric wafer transducer can be used for selective excitation of the S0 mode. A comparison of finite element simulations with experimental results showed that the more advanced models yield better agreement with experiment for the S0 mode. Some discrepancies between the simulated and measured A0 mode behavior has been attributed to inconsistencies in the transducer bonding in our experiments. Finally, the finite element simulations can be extended to explore important phenomena that occur in wafer transducers, including pulse dispersion and the dependence of transfer gain on the transducer thickness.

Acknowledgements

This work is partly supported by the National Science Foundation under Grant No.CMS-0329880, and the authors gratefully acknowledge that support. Any opinions, findings, and conclusions or recommendations expressed in this material are those of the authors and do not necessarily reflect the views of the sponsors.

References

[1] J.L. Rose, “Guided Wave Nuances for Ultrasonic Nondestructive Evaluation,” IEEE Trans. Ultrason., Ferroelec., and Freq. Control, vol. 47, 575-583 (May, 2000)
[2] M.J. Quarry and J.L. Rose, “Multimode guided wave inspection of piping using comb transducers,” Mater. Eval. 57, 1089-1090 (1999).
[3] J.L. Rose, S. Pelts, M. Quarry, “A comb transducer model for guided wave NDE,” Ultrason. 36, 163-168 (1998).
[4] W. Zhu and J.L. Rose, “Lamb wave generation and reception with time-delay periodic linear arrays: A BEM simulation and experimental study,” IEEE Trans. Ultrason., Ferroelec., and Freq. Control 46, 654-664 (1999).
[5] J. Li and J.L. Rose, “Implementing guided wave mode control by use of a phased transducer array,” IEEE Trans. Ultrasonics, Ferroelectrics, and Frequency Control 48, 761-768 (2001).
[6] Kessler S.S., Spearing S.M., Atalla M.J., Cesnik C.E.S. and C. Soutis. “Damage Detection in Composite Materials using Frequency Response Methods.” Proceedings of the SPIE’s 8th International Symposium on Smart Structures and Materials, 4-8 March 2001, Newport Beach, CA.
[7] V. Giurgiutiu and A.N. Zagrai, “Characterization of piezoelectric wafer active sensors,” Journal of Intelligent Material Systems and Structures 11, 959-975 (2000).
[8] Kessler S.S., Spearing S.M. and C. Soutis. “Structural Health Monitoring of Built-up Composite Structures using Lamb Wave Methods.” submitted for publication to Journal of Intelligent Material Systems and Structures.
[9] V. Giurgiutiu, “Lamb Wave Generation with Piezoelectric Wafer Active Sensors for Structural Health Monitoring,” Smart Structures and Materials 2003: Smart Structures and Integrated Systems, 111
[10] J.H. Nieuwenhuis, J. Neumann, D.W. Greve, and I.J. Oppenheim, ”Generation and detection of guided waves using PZT wafer transducers,” (in preparation).